Intensity-noise properties of injection-locked lasers

Charles C. Harb, Timothy C. Ralph, Elanor H. Huntington, Ingo Freitag,* David E. McClelland, and Hans-A. Bachor
Department of Physics, Faculty of Science, The Australian National University, Australian Capital Territory 0200 Australia
(Received 6 December 1995)

We present experimental results that illustrate how laser intensity noise near the quantum-noise limit is transferred in an injection-locked cw Nd:(yttrium aluminum garnet) nonplanar ring-oscillator laser. We show that these results are in extremely good agreement with our quantum-mechanical model describing the injection locking process [T. C. Ralph, C. C. Harb, and H.-A. Bachor, Phys. Rev. A]. Three regions in the intensity-noise spectrum are identified and we show that different minimum noise levels exist in these regions. Finally, we show that the injection-locked laser can generate and preserve nonclassical states. [S1050-2947(96)03110-1]

PACS number(s): 42.50.Lc, 42.55.Ah, 42.55.Xi, 42.60.Da

I. INTRODUCTION

Injection locking is an established field of research dating back to the 1960s [2]. Several reports have shown that it is possible to use a low power (hundreds of mW) diode pumped monolithic Nd:YAG (YAG denotes yttrium aluminum garnet) ring laser [3] (NPRO) to injection lock a high power (many W) Nd:YAG ring laser [4–7]. These reports verified that high power lasers could be controlled by low power lasers.

Fueled by the desire to develop ultrasensitive interferometric measurements, recent attention has focused on examining the transfer of intensity noise from the different noise sources in the laser system to the output of the injection-locked laser system [7–9]. These studies considered the basic behavior of the injection locking process in the large signal limit, hence their theories are not applicable to signals near the quantum-noise level.

In this paper, we wish to address the problem of how the intensity-noise spectrum of an injection-locked laser compares with the noise spectrum of an ideal quantum-noise limited laser of the same power. We present experimental results illustrating the noise transfer and compare these results with our fully quantum-mechanical theory [1]. The experimental and theoretical results show extremely good quantitative agreement.

Our model produces a single analytic expression relating the intensity-noise spectrum, for both the free-running and injection-locked lasers, to the known and measurable physical parameters of the Nd:YAG laser, as well as to the master and slave noise sources. Hence we show that it is possible to predict the intensity-noise spectrum of an injection-locked laser system.

Summary of the intensity-noise properties of injection locking

A conventional injection-locked laser system consists of a high power laser (the slave laser) which is locked to a low power, low noise laser (the master laser). Both these lasers are pumped by separate pump sources, as shown in Fig. 1.

Free-running solid-state laser systems, such as the diode pumped monolithic Nd:YAG ring lasers used in this work, have intensity noise associated with their output that is due to an interaction between the atoms in the lasing medium, the cavity storage rate, variations in the intracavity photon number introduced from the laser's pump source, and vacuum fluctuations. This noise can be reduced by injection locking [7,9].

Intensity noise filters through to the output of the injection-locked laser from the slave's pump lasers and from the master laser. We can view this intensity noise as being similar to a spectrum of amplitude modulation sidebands. A quantitative frequency description will be presented later in this paper. The transfer of intensity noise from these noise sources can be summarized as follows.

The slave laser acts like a low-pass filter to the noise of its pump source, as shown in the schematic diagram Fig. 2(a). The transfer of modulation from the slave's pump source through to the injection-locked slave output is characterized by minimal attenuation at dc (zero modulation frequency), followed by continuously increasing attenuation with the

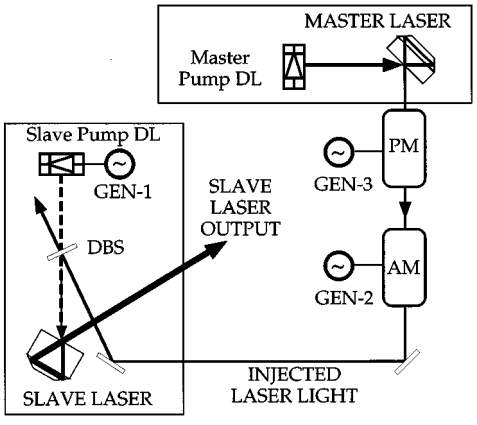

FIG. 1. Schematic diagram showing the basic elements of the injection locking system that is used in this work. The abbreviations are DL, diode laser; AM, amplitude modulator; PM, phase modulator; GEN, sinusoidal signal generator; and DBS, dichroic beam splitter.

*Present address: Laser Zentrum Hannover, Hollerithallee 8, D-30419 Hannover, Germany.

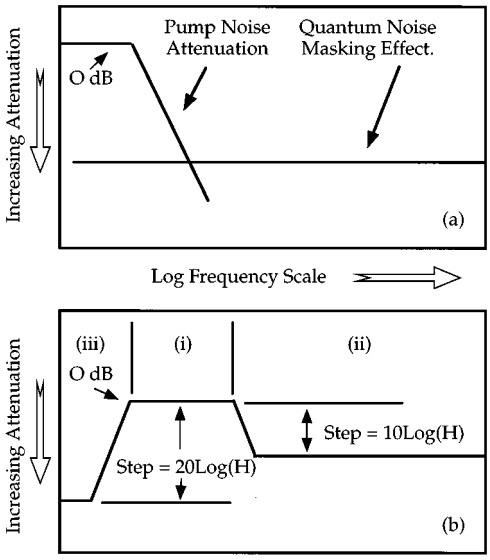

FIG. 2. Schematic diagram showing the expected signal transfer from (a) the slave's pump DL and (b) the master laser to the output of the injection-locked laser.

modulation frequency until the signals fall below the quantum-noise limit (QNL) of the slave laser. The rate of change of the attenuation, which determines the bandwidth of the low-pass filter, can be as high as 20 dB per decade. The corresponding corner frequency for this attenuation is determined by the characteristics of the slave laser as well as the intensity and detuning of the injected master radiation.

The transfer of modulation of the master laser through the injection-locked system is more complicated. It can best be described by discussing three distinct frequency regions [see Fig. 2(b)] in the output noise spectrum of the injection-locked laser system.

Let us start with the frequency region numbered (i) in Fig. 2(b). The output signal is an amplified version of the spectrum of the master laser. This is called the amplification region. In this region the slave acts like a linear optical amplifier to any modulation signals on the master laser. Both the modulation and the coherent fields are amplified, and consequently, beating between them produces an output signal which is amplified by the square of the power ratio of the master to the slave. Signals on the master retain their signal to noise ratio in the output of the locked slave if they are large compared to the QNL. However, for signals that are close to the QNL the signal to noise ratio is reduced. It should be noted that even if both the master and free-running slave lasers were QNL then the noise in this region would still be larger than the QNL. This increased noise level is due to the amplification of the quantum noise of the master. The bandwidth of this region is determined by the characteristics of the slave laser as well as the intensity and detuning of the injected master radiation, as is discussed later in this paper.

In the frequency region numbered (ii), there is neither attenuation nor amplification of the signal from the master laser. The modulation signal of the master laser is directly reflected off the cavity of the slave laser without entering. The reflected signal coherently beats with the strong slave beam and produces a modulation signal at the output which is greater in magnitude than the original modulation of the master by the power ratio. The noise floor is set by the noise level of the master laser and the signal to noise ratio at the output is identical to that of the master laser.

In the frequency region (iii), the slave laser is very strongly coupled to its pump source and hence marginally affected by modulations of the master laser. That is, the total output power of the slave laser system is determined by the slave's pump source and hence any forced oscillation from the external field cannot be amplified. This implies that the total output power of the injection-locked system is the geometric sum of the master and slave free-running optical powers, and hence near dc the response of the injection-locked laser to master noise fluctuations is also the geometric sum.

Semiclassical models have predicted the existence of regions (i) and (iii) in solid-state lasers [7,9] but not the correct response to small signals. Quantum-mechanical models have studied region (i) in semiconductor laser amplifiers [10], region (iii) in injection-locked semiconductor lasers [11], and regions (i) and (ii) in solid-state lasers [12]. In this paper we present a quantum-mechanical model that combines all three regions in the one formalism and demonstrate the existence of these regions experimentally using an injection-locked Nd:YAG NPRO laser.

In Sec. II of this paper we state the results of our theoretical model, the details of which are presented in [1]. We show in detail how the parameters in the theory can be determined from the experimentally available data. In Sec. III we describe the experimental arrangement used to generate the noise transfer functions. These results are compared with the theory in Sec. IV. Based on our theoretical model we predict, in Sec. V, the performance of an optimized injection-locked laser system that is subjected to nonclassical or sub-Poissonian pump and injected sources.

II. THEORY

We use the theory we have developed in Ref. [1] to describe this experiment. We quote the relevant results from that paper which are required to describe this type of laser system. We will also briefly summarize the basic concept of this theory, which is designed to predict the output noise spectrum of the laser as a function of the noise of the various input sources. Note that the theory contains the conventional parameters, such as intracavity laser amplitude and stimulated emission rate.

The atomic level scheme used in the model is a ''four-level'' scheme applicable to Nd ions. The upper-pump levels are assumed to have a very rapid decay and hence their dynamics are eliminated, as are the dynamics of the lasing coherence. We can thus approximate the ''four-level'' laser by a ''three-level'' laser. This is a good approximation for Nd:YAG, because γ_f is much larger than all the other decay rates. A schematic diagram for the energy level system of the lasers is given in Fig. 3. In this diagram we show the basic elements of the theory, the laser system, and how the active *atom-cavity* and *atom-cavity with injected field* systems couple together. We will be referring to this diagram throughout this paper as a basis for the explanations.

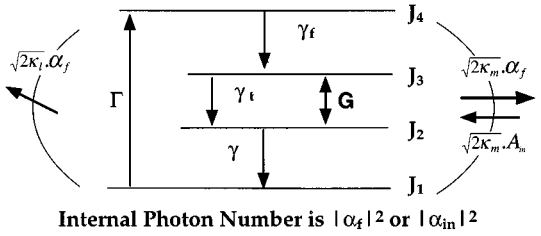

FIG. 3. Schematic of the energy level diagram for the ''four-level'' model used to describe the free-running and injection-locked systems. The variables are defined in the text.

The theory is based on a linearized input-output method to solve for the noise spectrum of the fluctuations around the steady-state output of the laser. The basic approach used here is to assume that we can write the intracavity amplitude operator $\hat{a}_f(t)$ of the free-running laser in the following standard linear form:

$$\hat{a}_f(t)=\alpha_f+\delta\hat{a}_f(t). \tag{1}$$

The circumflex indicates operators. α_f is the stable semiclassical steady-state intracavity amplitude of the free-running laser (which may be complex), and hence $|\alpha_f|^2$ is proportional to the output power of the laser system [see Eq. (29)]. $\delta\hat{a}_f(t)$ represents small fluctuations about this steady state, and all the quantum mechanics of the field is carried by these fluctuations.

We use the boundary condition at the output mirror to determine the output field:

$$\hat{A}_{\text{out}}=\sqrt{2\kappa_m}\hat{\alpha}_f-\hat{A}_{\text{in}}, \tag{2}$$

where $\sqrt{2\kappa_m}$ is proportional to the amplitude transmission of the output mirror, as given in Eq. (27), and has units $\text{s}^{-1/2}$. $\hat{A}_{\text{out}}$ and $\hat{A}_{\text{in}}$ are the amplitude operators for the external fields exiting and entering the laser cavity at the mirror. The amplitude of $\hat{A}_{\text{in}}$ can either be zero for a vacuum mode or be nonzero for the case of an injected laser field. $\hat{A}_{\text{out}}$ and $\hat{A}_{\text{in}}$ have the units $\text{photons}^{1/2}\text{s}^{-1/2}$, and represent the amplitude of the laser field external to the laser cavity. There are fluctuations associated with $\hat{A}_{\text{in}}$ irrespective of its amplitude, and they may have non-Poissonian statistics (this will be discussed in Sec. V).

If we consider just the semiclassical steady state then we find that Eq. (2) implies

$$A_{\text{out}}=\sqrt{2\kappa_m}\alpha_f \tag{3}$$

for a free-running laser, as there is no input field, or

$$A_{\text{out}}=\sqrt{2\kappa_m}\alpha_f-A_{\text{in}} \tag{4}$$

for an injection-locked laser. Similarly, the output fluctuations of the laser are given by

$$\delta\hat{A}_{\text{out}}=\sqrt{2\kappa_m}\delta\hat{a}_f-\delta\hat{A}_{\text{in}}. \tag{5}$$

In the case of a free-running laser, $\delta\hat{A}_{\text{in}}$ are vacuum fluctuations which are nonzero. In an injection-locked laser $\delta\hat{A}_{\text{in}}$ are the fluctuations of the master.

Just as α_f can be calculated from the dynamics of the active atoms and the input power of the pump, so too $\delta\acute{x}aq_f$ can be calculated from the dynamics of the atoms and the input fluctuations of the pump and the various other vacuum fields associated with spontaneous emission, dipole fluctuations, and losses. In this way the noise spectrum of the fluctuations can be calculated analytically in terms of the noise spectra of the various inputs. The details of these calculations can be found in Ref. [1].

The injected field, A_{in}, produces a mode inside the cavity, α_{in}, that obeys the relations

$$\alpha_{\text{in}}=\begin{cases}\dfrac{A_{\text{in}}}{\sqrt{2\kappa_m}} & \text{far from cavity resonance}\\[2ex] \dfrac{\mathcal{G}A_{\text{in}}}{\sqrt{2\kappa_m}} & \text{near cavity resonance}\end{cases} \tag{6}$$

where $\mathcal{G}$ is the intracavity gain of the laser, and is a complicated function that is dependent on many parameters. Determination of the steady-state behavior of the injection-locked laser system is accomplished using the following set of semiclassical equations:

$$\dot{\alpha}_f^2=0=\frac{G}{2}(J_3-J_2)\alpha_f^2-\kappa\alpha_f^2, \tag{7a}$$

$$\dot{\alpha}_{\text{in}}^2=0=\frac{G}{2}(J_3-J_2)\alpha_{\text{in}}^2-(\kappa+\imath\Delta)\alpha_{\text{in}}^2+\sqrt{2\kappa_m}A_{\text{in}}, \tag{7b}$$

$$\dot{J}_2=0=G(J_3-J_2)(\alpha_f^2+|\alpha_{\text{in}}|^2)+\gamma_t J_3-\gamma J_2, \tag{7c}$$

$$\dot{J}_3=0=-G(J_3-J_2)(\alpha_f^2+|\alpha_{\text{in}}|^2)-\gamma_t J_3+\Gamma J_1, \tag{7d}$$

$$J_1+J_2+J_3=N, \tag{7e}$$

where $\imath=\sqrt{-1}$, the J_i are the atomic population in the ith levels, N is the number of active atoms which is generally normalized to 1 for ease of calculation and then rescaled back as described in Sec. IV A, Eqs. (28) and (29). The other parameters used in the model are Γ, the pump rate; γ, the decay rate from the lower lasing level; γ_t, the spontaneous emission rate between the lasing levels; $2\kappa_m$, the cavity photon decay rate due to the input-output mirror; $2\kappa_l$, the cavity photon decay rate due to losses; $2\kappa=2\kappa_m+2\kappa_l$, the total cavity photon decay rate; and G, the stimulated emission rate. It should be noted that all the parameters defined in this paragraph are constants for a given laser system, except for Γ, which determines the intracavity amplitude and consequently the output power of the laser. Hence knowledge of Γ is necessary if we wish to model the laser. The detuning between the injected mode and slave cavity mode is Δ [13].

The injected field can have any phase, hence we take it to be real. Notice that this forces the locked mode to be complex for all but zero detunings. An examination of the behavior of the semiclassical steady state as a function of the detuning between the injected field and the cavity resonance reveals the standard injection locking behavior, which is discussed in more detail in Refs. [1,7,9]. At large detunings between the master and a slave cavity mode there is very

little buildup of the injected field in the laser cavity and hence negligible interaction with the active atoms. The output of the laser is just the geometric addition of the master and slave fields. As the detuning is reduced the injected field intracavity intensity increases and starts to rob gain from the free-running mode, causing the free-running slave mode to drop in intensity. Eventually, when the gain to loss balance of the locked mode equals that of the free-running mode, the free-running mode is extinguished. From Eqs. (7a) and (7b) we see that this occurs when

$$\Delta_l = \sqrt{2\kappa_m}\frac{A_{\rm in}}{|\alpha_f|} \cong \sqrt{2\kappa_m}\frac{A_{\rm in}}{\alpha_{\rm in}}. \tag{8}$$

The detuning Δ_l is called the locking range and α_f is the steady-state amplitude of the free-running slave laser internal field with no injected field. For detunings less than the locking range the free-running slave mode does not oscillate and is replaced by the mode of the master laser, as would be the case in an optical amplifier. However, the intensity-noise properties of the injection-locked laser differ from those of an optical amplifier.

For simplicity we have assumed that the locking range and cold cavity linewidth are much larger than the stimulated emission rate, pump rate, and spontaneous emission rate, i.e.,

$$\Delta_l, \kappa \gg G\alpha_{\rm in}^2, \Gamma, \gamma_t. \tag{9}$$

This is a reasonable assumption for solid-state lasers.

The amplitude quadrature fluctuation is defined by $\delta\hat{X}_{\rm out} = \delta\hat{A}_{\rm out} + \delta\hat{A}_{\rm out}^{\dagger}$ The intensity-noise spectrum $V_{\rm out}(\omega)$ is the spectral variance of the Fourier transform of $\delta\hat{X}_{\rm out}$. From an experimental point of view, this means that

$$V_{\rm out}(\omega) = \frac{\Delta P_{\rm out}(\omega)^2/P_{\rm out}}{\Delta P_{\rm QNL}^2/P_{\rm out}}, \tag{10}$$

where $P_{\rm out}$ is the steady-state optical power of the laser system, $\Delta P_{\rm QNL}^2$ is the laser's spectral variance due to quantum-noise limited fluctuations when operating with output power $P_{\rm out}$ and $\Delta P_{\rm out}(\omega)^2$ is the measured spectral variance of the laser. For all the variables in this work we assume that the spectral variance is referred to the full power of their respective lasers. In this terminology $V_{\rm out}(\omega) = 1$ implies that the laser fluctuations are limited by quantum noise. If the laser radiation experiences optical attenuation, or the detected power is less than the full power of the laser system, then the relations discussed in Sec. IV [i.e., Eq. (25)] must be used to rescale the variables to the observed spectral variance.

A. The free-running laser

In the case where the injected master field becomes the vacuum field, i.e., $\alpha_{\rm in} = A_{\rm in} = 0$, then the intensity-noise spectrum for the free-running laser is V_f as derived in Ref. [1]:

$$\begin{aligned} V_f = 1 + \{&4\kappa_m^2(\omega^2+\gamma_l^2) - 4\kappa_m\omega_r^2\gamma_l \\ &+ 2\kappa_m G^2\alpha_f^2(\Gamma J_1 V_p + \gamma_t J_3) + 2\kappa_m G[(\gamma_t+\Gamma)^2+\omega^2] \\ &\times(J_3+J_2) + 4\kappa_m\kappa_l(\gamma_l^2+\omega^2)\}/\{(\omega_r^2-\omega^2)^2+\omega^2\gamma_l^2\}, \end{aligned} \tag{11}$$

where

$$\begin{aligned} \omega_r &= \sqrt{G^2\alpha_f^2(J_3-J_2)} \\ &= \sqrt{2\kappa G\alpha_f^2} \end{aligned} \tag{12}$$

and

$$\gamma_l = G\alpha_f^2 + \gamma_t + \Gamma. \tag{13}$$

V_f relates the output intensity-noise spectrum to the slave's pump source intensity-noise spectrum V_p. V_f shows the existence of the well known resonant relaxation oscillation (RRO) which is defined in Eq. (12). γ_l is a parameter that determines the damping of this natural oscillation. The relations given in Eq. (7) allow us to rewrite Eq. (12) into the form

$$\begin{aligned} \omega_r &= \sqrt{2\kappa\gamma_t}\sqrt{\frac{\Gamma}{\Gamma_{\rm th}}-1} \\ &= \sqrt{\frac{1}{\tau t_c}}\sqrt{\frac{P_{\rm pump}}{P_{\rm th}}-1}, \end{aligned} \tag{14}$$

where $\Gamma_{\rm th}$ is the pump rate at the lasing threshold, τ is the spontaneous lifetime of the upper lasing level, t_c is the cavity lifetime, $P_{\rm pump}$ is the pump power, and $P_{\rm th}$ is the pump power at threshold. We use the relation given in Eq. (12), instead of that given in Eq. (14), to determine the intracavity photon number because there is large experimental uncertainty in determining $P_{\rm th}$ directly. This will be discussed in more detail in Sec. IV A.

Examination of the intensity noise of the free-running laser, as described by V_f, reveals that below the RRO frequency the pump noise, the quantum noise due to spontaneous emission, and dipole fluctuations appear in the output intensity-noise spectrum. Above the RRO frequency the magnitude of these noise sources passing through to the output intensity-noise spectrum decreases due to the filtering effect of the cavity. In the limit of high frequencies the spectrum tends to 1, indicating that the laser is quantum-noise limited at high frequencies. All these features are observed experimentally, see Sec. IV A.

B. The injection-locked laser

The intensity-noise spectrum of the output light for an injection-locked laser, V_l, is given by (master field nonzero)

$$\begin{aligned} V_l = V_{\rm in} + \{&4V_{\rm in}\kappa_m^2(\omega^2+\gamma_{L\ {\rm in}}^2) - 4V_{\rm in}\kappa_m\omega_R^2\gamma_{L\ {\rm in}} \\ &- 4V_{\rm in}\kappa_m\omega^2\Delta_l + 2\kappa_m G^2\alpha_{\rm in}^2(\Gamma J_1 V_p + \gamma_t J_3) \\ &+ 2\kappa_m G[(\gamma_t+\Gamma)^2+\omega^2](J_3+J_2) \\ &+ 4\kappa_m\kappa_l(\gamma_{L\ {\rm in}}^2+\omega^2)\}/\{(\omega_R^2-\omega^2)^2+\omega^2\gamma_L^2\}, \end{aligned} \tag{15}$$

where

$$\omega_R=\sqrt{[G^2\alpha_{\rm in}^2(J_3-J_2)+\Delta_l\gamma_{L\ \rm in}]}$$
$$\cong\sqrt{G^2\alpha_{\rm in}^2(J_3-J_2)}=\omega_r \tag{16}$$

and

$$\gamma_L=(G\alpha_{\rm in}^2+\gamma_t+\Gamma+\Delta_l)$$
$$=\gamma_{L\ \rm in}+\Delta_l$$
$$\cong\Delta_l>\gamma_l\,. \tag{17}$$

This set of relations shows that both the natural resonance (the RRO) and the damping factors are altered by the injected field. That is, $\omega_r \Rightarrow \omega_R$ and $\gamma_l \Rightarrow \gamma_L$. The increased damping created as a result of the injected field ensures that the RRO does not oscillate unless the injected field is of the same magnitude or smaller than the losses in the cavity.

For the relations presented above we have assumed that the injected field is resonant with the slave cavity. The solution for the case where the injected field is not resonant with the slave cavity mode is discussed in detail in Ref. [1]. This latter case is beyond the scope of this present work.

C. Transfer of slave pump source noise to the injection-locked laser

Consider the case where the pump noise is the dominant noise source, i.e., $V_p \gg V_{\rm in},1$. Then Eq. (15) can be simplified to

$$V_l=\frac{(2\kappa_m G^2\alpha_{\rm in}^2\Gamma J_1 V_p)}{[(\omega_R^2-\omega^2)^2+\omega^2\gamma_L^2]}\,. \tag{18}$$

The injection-locked slave laser acts like a low-pass filter to the noise originating from its pump source. At frequencies much lower than the RRO frequency, the pump noise of the injection-locked laser is virtually the same as for the free-running laser [see Eq. (24)]. The physical reason for this effect is that the slave laser's output power is strongly coupled to slow variations in its pump source total output power. This coupling starts to decrease as the pump source fluctuations become more rapid. The corner frequency $\omega_{c\,\rm low}$ for this coupling is given by the relation

$$\omega_{c\,\rm low}=\frac{\omega_R^2}{\gamma_L}\cong\frac{\omega_R^2}{\Delta_l}. \tag{19}$$

From the frequency $\omega_{c\,\rm low}$ to approximately γ_L the roll off is proportional to ω^{-2}. At higher frequencies, the cavity also produces a roll off and hence the roll off is proportional to ω^{-4}.

D. Transfer of master laser noise to the injection-locked laser

Now we consider the noise transfer from the master laser to the output of the locked system. In particular, the situation where the master noise is similar to that of the slave laser pump noise, i.e., $V_{\rm in}=V_p$, so that we can identify the frequency dependence. We can identify three distinct frequency regimes in Eq. (15).

(i) Amplification regime (refer to Fig. 2(b). In the frequency region close to the slave's RRO the injected fluctuations are amplified. If we simplify the relation for the spectrum [Eq. (15)] by using Eq. (9) and assuming that we are at a frequency close to that of the free-running RRO we find

$$V_l\cong V_{\rm in}\left(1+\frac{2\kappa_m\alpha_{\rm in}^2}{A_{\rm in}^2}-\frac{2\sqrt{2\kappa_m}\alpha_{\rm in}}{A_{\rm in}}\right)+\frac{G(J_3+J_2)\alpha_{\rm in}^2}{A_{\rm in}^2}$$
$$\cong V_{\rm in}H+(H-1)+\frac{4\kappa_l\alpha_{\rm in}^2}{A_{\rm in}^2}, \tag{20}$$

where

$$H=\frac{(\sqrt{2\kappa_m}\alpha_{\rm in}-A_{\rm in})^2}{A_{\rm in}^2}\equiv\frac{P_{\rm in}+P_f}{P_{\rm in}}\equiv\frac{(\text{optical power out})}{(\text{optical power in})} \tag{21}$$

is the semiclassical intensity amplification factor, with $P_{\rm in}$ and P_f being the injected master power and free-running slave optical powers. In deriving Eq. (20) we have also used the fact that, in the presence of rapid decay from the lower lasing level, $J_3 \gg J_2$, to simplify the second term. The first two terms of Eq. (20) are the standard result for the intensity-noise spectrum of a linear optical amplifier [14], where the injected fluctuations are amplified by the semiclassical amplification factor. The third term in Eq. (20) represents the effect of quantum fluctuations, introduced by the phase decay of the lasing coherence, and the intracavity losses on the intensity-noise spectrum. These effects have previously been noted for semiconductor lasers [10].

(ii) High frequency regime. If we move to frequencies much higher than the resonance the amplification rolls off (the corner frequency for this roll off is at $\omega_{c\,\rm high}\approx\Delta_l$) until at frequencies

$$\omega\gg\sqrt{\frac{V_{\rm in}\kappa_m^2+4\kappa\kappa_m}{V_{\rm in}}} \tag{22}$$

we find

$$V_l\cong V_{\rm in}\,. \tag{23}$$

Physically, we are outside the laser cavity linewidth, hence high frequency fluctuations inside the cavity are suppressed while high frequency fluctuations on the injected field are simply reflected off the front mirror.

(iii) Low frequency regime. If we examine the frequencies lower than the slave's RRO we also get a roll off of the amplification of the fluctuations of the injected field as we move toward zero frequency. In addition pump noise and other noise sources associated with the free-running dynamics of the slave laser roll on. If we add the extra condition that we are well above threshold ($G\alpha_{\rm in}^2\gg\Gamma\gg\gamma_t$) and consider frequencies very close to dc ($\omega\approx 0$) then Eq. (15) becomes

$$V_l\cong\frac{V_{\rm in}A_{\rm in}^2+V_p\Gamma J_1}{(\sqrt{2\kappa_m}\alpha_{\rm in}-A_{\rm in})^2}\cong\frac{P_{\rm in}V_{\rm in}+P_fV_f}{P_{\rm in}+P_f}, \tag{24}$$

where we have used the fact that far above threshold, with rapid decay from the lower lasing level, $J_1 \cong 1$ and hence energy conservation demands $\Gamma J_1 \cong 2\kappa_m \alpha_{\text{in}}^2$ Under these same assumptions the spectrum of the free-running slave [Eq. (11)] is just determined by the pump noise (i.e., $V_l = V_p$). Hence at low frequencies the output spectrum is just the geometric addition of the fluctuations of the injected and internal modes and is similar to the spectrum when the lasers are not locked.

III. EXPERIMENT

In this section we will describe the experimental setup used to investigate injection locking. All the experimental results presented in this paper are obtained using diode pumped nonplanar Nd:YAG ring lasers operating at 1064 nm [3,8]. The master laser is a 200 mW output laser with external intensity feedback control (LightWave 122) [15,16] that eliminates the RRO from this laser. The slave laser [8] generates an output power of more than 700 mW, but has no suppression of its RRO.

These lasers have active temperature control of their Nd:YAG crystals. The stability of the lasers' temperature is of the order of 1 mK over periods of several seconds. This is crucial because a 1 mK temperature change can alter the output frequency by several MHz, and hence limit the ability to injection lock. It is possible to temperature tune the frequency of the master laser over several tens of GHz. This encompasses many longitudinal modes of the slave laser, all of which will lock to the master [13]. All our results are obtained by locking to the central free-running mode.

The experimental setup contains two distinct sections. Figure 1 illustrates the basic optical arrangement for the injection of the master field into the slave laser cavity. The master light is directed into the slave cavity using a dichroic beam splitter (DBS) that is placed in the path between the pump diode lasers and the Nd:YAG crystal. This beam splitter has high transmission at the pump diode wavelength (808 nm) $>95\%$ and high reflectance at the Nd:YAG wavelength (1064 nm) $>95\%$. Thus both maximal pumping and injection can be achieved. After passing through mode matching and isolation optics, the master light passes through a set of polarizing and polarization rotating optics (these optical components are not shown in the diagram). This allows adjustment of the master power and polarization before entering the slave. The polarization is chosen to most closely match the intracavity eigenmode of the free-running slave laser (this is discussed further in Ref. [17]).

Phase and amplitude modulation of the master is accomplished using two electro-optic modulators (PM and AM, respectively). Modulation of the pump diode laser light is accomplished by directly modulating the current of the diode laser. A sinusoidal signal is coupled into the diode laser current and the resulting modulation is detected on the output of the Nd:YAG laser.

Figure 4 is a schematic of the diagnostic system used in this experiment. A power meter is used to monitor the powers of the slave, master, and locked system for each set of data taken. Two identical transimpedance low noise photodiodes (PD3 and PD4), with bandwidths of dc to 20 MHz, and an rf spectrum analyzer (SA) were used in a balanced

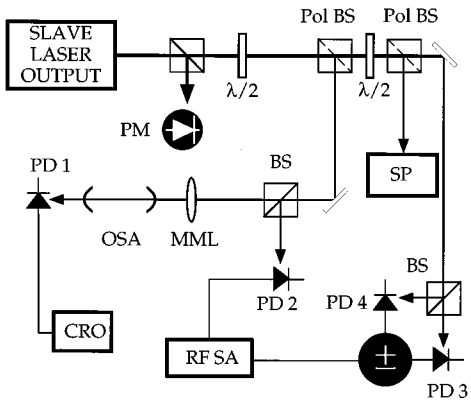

FIG. 4. Schematic diagram of the diagnostics used to monitor the output of the injection-locked system. The abbreviations are MML, mode matching lens; λ/2, 1064 nm half wave plate; Pol BS, polarizing beam splitter; BS, beam splitter (50/50); RF SA, radiofrequency spectrum analyzer; CRO, cathode ray oscilloscope; ±, adding and subtracting electronics; OSA, optical spectrum analyzer; SP, spectrometer with charge-coupled device (CCD) array; and PD, radiofrequency photodetector.

detection system to make noise measurements. All the noise measurements were made with 1.70 ± 0.05 mW (inferred) of detected optical power, split between the two photodetectors. The locking range was determined by observing the disappearance of the beat signal between master and free-running slave with these detectors.

The transfer function measurements were obtained by observing the magnitude of the AM signals on the lasers before and after injection locking using two transimpedance photodetectors with bandwidths of dc to 20 MHz and 10 kHz to 150 MHz, and an rf network-spectrum analyzer capable of a logarithmic frequency sweep.

It was also useful to monitor the injection-locked mode frequency with respect to the slave cavity frequency. This gave information as to whether or not the oscillating mode was at cavity resonance or at some other frequency inside the locking bandwidth. We used the well known Pound-Drever technique (see [18] for more details) to estimate the detuning between the master and slave cavity modes. This involves placing an rf phase modulation on the master radiation and demodulating the signal reflected off the slave cavity. The signal obtained, called the error signal, gives a cavity-detuning-dependent voltage.

IV. RESULTS AND COMPARISON WITH THEORY

A. Noise spectrum of the free-running slave

Figure 5 shows the noise spectrum of the free-running slave operating at an output power of 400 ± 5 mW, with a detected optical power of 1.70 ± 0.05 mW. The spectrum is shown normalized to the QNL for the same detected power. Overlaid is the corresponding theoretical curve [from Eq. (11)] where optical attenuation of the laser field is taken into account via

$$V_{\text{obs}} = 1 + \eta(V_f - 1), \tag{25}$$

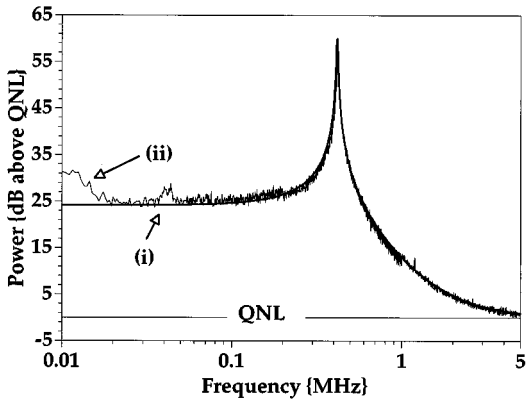

FIG. 5. The resonant relaxation oscillation (RRO). (i) Theoretical noise spectrum calculated using the measured parameters of the experiment. (ii) Experimental results of the intensity-noise spectrum for the slave laser system operating with an output power of 400 mW and RRO frequency of 420 kHz and a detected optical power of 1.7 mW.

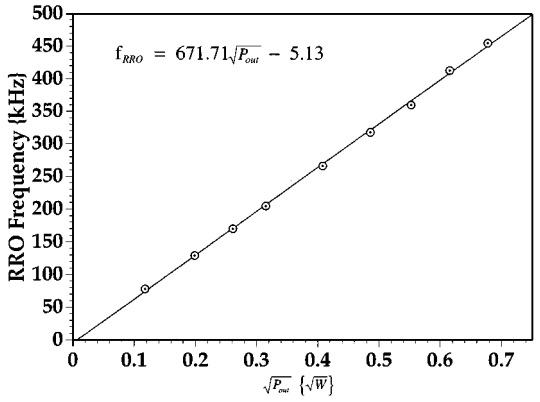

FIG. 6. Experimental results of the variation of the position of the RRO as a function of the output intensity.

where the detection efficiency $\eta = (1.7\ \text{mW}/400\ \text{mW}) = 0.004$. We note that the two curves demonstrate excellent agreement between the theory and the experimental results. The important aspect to note is that the model predicts the magnitude of the noise equally well for signals near QNL and also many dB above QNL.

Generation of the curve shown in Fig. 5 required the following procedure. The parameters used in calculating V_f are

$$G = \sigma_s c \rho = 6.6 \times 10^{11}\ \text{s}^{-1},$$
$$\gamma = 3.3 \times 10^{7}\ \text{s}^{-1},$$
$$\gamma_t = 4.3 \times 10^{3}\ \text{s}^{-1}, \tag{26}$$

where σ_s is the stimulated emission cross section, c is the speed of light in the medium, and ρ is the atomic density of the lasing atoms [19]. The round-trip losses in the crystal are quoted as $L = 1.6\%$ while the output coupling at the polarization of the free-running mode is quoted as $T = 2.5\%$. Hence

$$2\kappa_l = \frac{Lc}{ln} = 9.3 \times 10^{7}\ \text{s}^{-1},$$
$$2\kappa_m = \frac{Tc}{ln} = 1.5 \times 10^{8}\ \text{s}^{-1}, \tag{27}$$

where l is the round-trip length, which is equal to 28.54 mm in this case, and n is the refractive index of the laser material at 1064 nm, which is equal to 1.818. These parameters are particular to our diode pumped Nd:YAG nonplanar ring oscillator. G, $2\kappa_m$, and $2\kappa_l$ can vary for other laser systems because ρ, L, and T may differ.

The two remaining parameters required to model the laser are Γ and V_p. These are fitted to the experimental data. As previously discussed, an accurate value of Γ is required for the determination of the laser's operating power above threshold, i.e., the intracavity photon number α^2. Γ is chosen such that the RRO frequency predicted by the model corresponds to the RRO frequency measured experimentally. To do this we solve the relations in Eq. (7) and adjust Γ till the appropriate RRO frequency is located. The value for Γ is generally calculated numerically as a simple analytic expression that relates Γ to the J_i's and α is not possible to obtain.

We determine N by experimentally measuring the RRO frequency as a function of the output power of the laser. This information relates α to the output power, and then N can be determined in the following manner: Eq. (12) relates the RRO frequency, f_{RRO} in Hz, to the output optical laser power P_{out} by

$$f_{\text{RRO}} = \frac{\omega_r}{2\pi} = \frac{1}{2\pi}\sqrt{\frac{\kappa G}{\kappa_m N h \nu}}\sqrt{P_{\text{out}}}, \tag{28}$$

where h is Plank's constant, ν is the optical frequency, $h\nu = 1.868 \times 10^{-19}$ J, and

$$P_{\text{out}} = N h \nu A_{\text{out}}^2 = 2\kappa_m N h \nu \alpha_f^2. \tag{29}$$

In Fig. 6 we plot experimental data that show the variation of f_{RRO} as a function of $\sqrt{P_{\text{out}}}$. The curve is linearly dependent on $\sqrt{P_{\text{out}}}$, in agreement with the relation given in Eq. (28). From the slope of Fig. 6 we obtain a value for the number of active atoms N of 3.2×10^{17}. As a rough comparison we can calculate the expected number of lasing atoms by estimating the number of Nd:YAG atoms in the laser mode from the known doping of the material. We assume that the volume is a cylinder of radius 240 μm (which is the output spot size of the laser) and is 5 mm long (which is the approximate pump length in the material), and this material has a Nd doping of 1.25×10^{20} atoms/cm^3, which gives a value of 1×10^{17} active atoms. This estimate suggests that the value calculated above is reasonable for this system.

We can now calculate the remaining parameters under the slave laser's operating condition of 400 mW of output power and a RRO frequency of 420 kHz. The spectral density is shown in Fig. 5 with its corresponding theoretical fit. The Γ that corresponds to a RRO frequency of 420 kHz is 12.3 s^{-1} per atom. This is consistent with the estimated absorbed pump power of 1.0 W. The intracavity photon number α^2 at

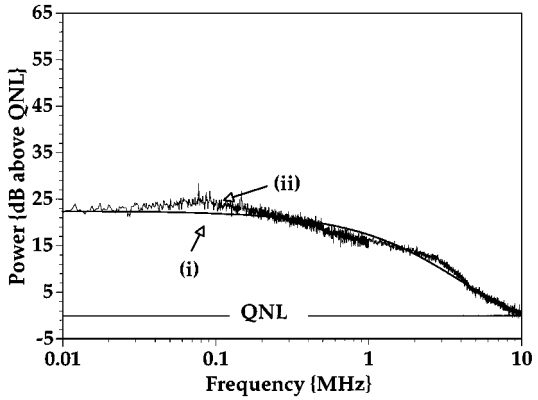

FIG. 7. The spectral intensity noise of the master laser. (i) Calculated best fit curve to the experimentally measured intensity-noise spectrum. (ii) Experimental results of the intensity-noise spectrum for the master laser system operating with an output power of 200 mW and a detected optical power of 1.7 mW. The intensity noise in the frequency regime near the master's RRO has been reduced by electronic feedback.

this pump power is 4.0×10^{-8} photons per atom and the populations of the energy levels are $J_1=3.199\times10^{17}$ atoms; $J_2=1.2\times10^{11}$ atoms; and $J_3=1.3\times10^{14}$ atoms.

The final parameter that is required is V_p. We find the best fit between theory and experiment is obtained by setting $V_p=500\,000$, i.e., 57 dB above the QNL. This is consistent with the measured intensity noise of the diode array for the power absorbed by the NPRO.

Having established that the model correctly describes the free-running slave, we now consider the injection-locked slave laser.

B. Injection-locked laser

1. The master intensity-noise spectrum

In our previous injection locking experiments [8] we found that the output noise level of the injection-locked slave was an amplified version of the injected master's spectrum. This is what would be expected in the amplification regime. The other noise regions could not be identified because the master laser's intensity-noise spectrum was comparable in magnitude to that of the slave's. In this set of experiments we use a master laser with an electronic intensity noise eater which reduces its spectral noise. The master noise is thus quieter than that of the slave in the frequency regime of the slave's RRO. Figure 7 shows the noise spectrum of the master laser with respect to QNL, with 1.7 mW of optical power on the detectors. Also shown is a polynomial fit to the experimentally measured intensity spectrum.

The mathematical form of the fit is

$$V_{\rm in}(\omega)=Z\,\exp\left(\frac{-0.024\omega^3+0.58\omega^2-5.71\omega+21.42}{10}\right), \tag{30}$$

where ω is the angular frequency and Z is a scaling constant set by the ratio of measured noise to the actual noise entering the laser. We will use this model of the master noise level to represent $V_{\rm in}$ in our theory.

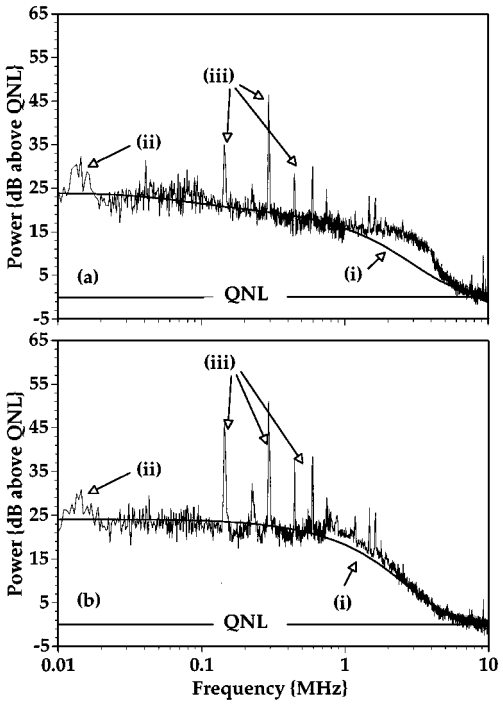

FIG. 8. The spectral intensity noise of the injection-locked laser. (a) shows the noise for the case $H=12.5$ and (b) shows the noise for the case where $H=75$. (i) A polynomial fit to the noise spectrum. (ii) Experimental results of the intensity-noise spectrum with a detected optical power of 1.7 mW. (iii) Excess noise due to optical amplification of the master laser's phase noise by the injection-locked slave laser.

It should be noted that the master and slave noise levels below approximately 10 kHz are of comparable magnitude for the detected photo current in our balanced detection system. The implication of this is that the locked noise level will appear unchanged at these frequencies, as will be discussed shortly.

2. The injection-locked intensity-noise spectrum

Figure 8 shows the intensity-noise spectrum of the injection locked system with respect to QNL, with 1.7 mW of optical power on the detectors. The slave laser is operating under the same conditions as for the free-running case. The theoretically generated curves shown use the parameters for the free-running slave laser and the theory fit for the master to determine the output noise level for the injection-locked system. This theory fit is appropriately scaled for the amount of injected power, using Eq. (25).

The injected power, i.e., the amount of master light launched into the slave cavity mode, is determined from the locking range, Δ_l. Equation (8) can be written in terms of input and output powers ($P_{\rm in}$ and $P_{\rm out}$) as

$$\Delta_l=\sqrt{2\kappa_m}\frac{A_{\rm in}}{|\alpha_f|}\cong 2\kappa_m\eta\frac{\sqrt{P_{\rm in}}}{\sqrt{P_{\rm out}}}, \tag{31}$$

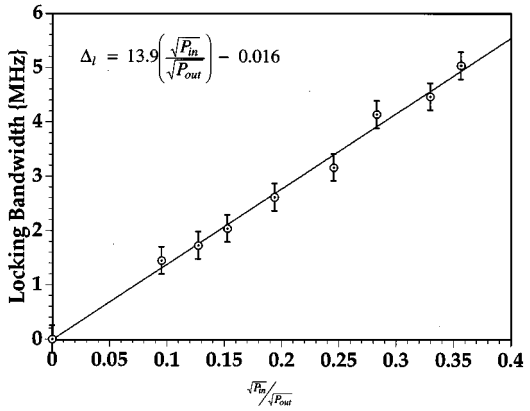

FIG. 9. Experimental results showing the locking range dependence on the ratio: square root (input power to output power).

where η is an experimentally determined constant that indicates how well the master radiation is coupled to the slave cavity. Figure 9 shows the variation of the locking range (Δ_l is converted to Hz) as a function of ($\sqrt{P_{\rm in}}/\sqrt{P_{\rm out}}$). The relationship is linear as expected. The slope of the graph is $2\kappa_m\eta = 2\pi\times 13.9\times 10^6$ rad s^{-1}. Given that the output coupler has a transmission of $\approx 3\%$ then we obtain that $\eta\approx 0.5$, and hence only 50% of the master field is passing into the slave cavity.

The two noise spectra that are presented here are for two different injected master field amplitudes. That is, for Fig. 8(a) $H\approx 12.5$ with locking range 3.5 MHz and for Fig. 8(b) $H\approx 75$ with locking range 1.9 MHz. We present the two to illustrate the noise is indeed dependent on the magnitude of the injected field. Furthermore, the theoretical fit is excellent for both cases.

The injection-locked noise spectrum is very different from the free-running case, shown in Fig. 5. The RRO is no longer present, and the overall noise levels are similar to that of the master [Fig. 8(b)]. In the *amplification region* [region (i) in Fig. 2(b)], with equal powers of master and locked slave detected, we expect equal noise levels in the master and locked spectra, provided that the noise is well above QNL. This is due to the effect of optical attenuation: the observed master spectrum is

$$\begin{aligned} V_{{\rm obs},m} &= 1+\eta_1(V_{\rm in}-1) \\ &\cong \eta_1 V_{\rm in}, \quad V_{\rm in}\gg 1 \end{aligned} \tag{32}$$

where $\eta_1=(1.7\ {\rm mW})/P_{\rm in}$. The observed locked slave spectrum is

$$\begin{aligned} V_{{\rm obs},l} &= 1+\eta_2(V_l-1) \\ &= 1+\eta_2\{[V_{\rm in}H+(H-1)]-1\}\cong \eta_2 H V_{\rm in}, \quad V_{\rm in}\gg 1 \end{aligned} \tag{33}$$

where $\eta_2=(1.7\ {\rm mW})/P_{\rm out}$, however, $\eta_1/\eta_2=H$, so $V_{{\rm obs},m}=V_{{\rm obs},l}$.

At *high frequencies* (beyond ≈ 4 MHz) [region (ii) in Fig. 2(b)] the locked slave laser has a noise level that is lower than the master level, due to the roll off of the amplification.

At *low frequencies* (below ≈ 400 kHz) [region (iii) in Fig. 2(b)] the locked slave laser has a noise level that is higher than the master level, approaching the noise level of the unlocked slave near zero frequency. This is due to slave pump noise affecting the locked system.

Other differences between the master noise level and that of the locked slave are noise peaks that appear at low frequency and some excess noise at ≈ 3 MHz [indicated by the label (iii) in Fig. 8]. These intensity-noise peaks in the injection-locked noise spectrum are not present in the intensity-noise spectrum of either of the free-running lasers. Excess noise can appear in the intensity-noise spectrum of the slave laser when detunings (of the master from the slave cavity resonance) are present [1]. In particular, phase noise of the master can couple into the intensity-noise spectrum. This effect is well known in empty cavities where detunings can be used to rotate the noise quadrature of the reflected light [20]. Similarly, pump phase noise can couple into the intensity-noise spectrum when detunings are present in second harmonic generation [21]. Hence we attribute these peaks to amplification of the master phase noise by the slave laser. From independent tests we have found that the master does have phase noise at the frequencies shown here. The high frequency excess noise is attributed to the injected mode frequency being detuned from the slave cavity resonance [1]. The excess noise can be dramatically altered by detuning the relative master laser frequency within the injection locking bandwidth.

C. Intensity-noise transfer functions

The structure appearing in the locked slave intensity-noise spectrum is a mixture of slave pump noise and master noise. In this section we examine the contribution from each individually by measuring the intensity-noise transfer functions.

The intensity-noise transfer functions

Figure 10 shows the transfer functions for the two power ratios given above. Also shown is the predicted transfer function for their respective experimental parameters.

For the pump transfer function, there is good agreement between the theoretical and experimental results for both power ratios [curves (i) and (ii), respectively]. The results show that low frequency signals originating at the pump of the slave are transmitted to the output of the injection-locked system almost unattenuated. The corner frequencies are at 40 kHz for $H\approx 12.5$ and 190 kHz for $H\approx 75$. However, the corner frequency $\omega_{c\,\rm low}$ for the higher power ratio is not predicted accurately due to experimental uncertainty of the master frequency within the locking bandwidth. The subsequent roll off with increasing frequency is at a predicted rate of $\approx$ 20 dB/decade, to the point where the results merge into the background noise level.

The master transfer functions are also shown in Fig. 10. Once again there is good agreement between the theoretical and experimental results [curves (iii) and (iv), respectively]. The results clearly show the three frequency regimes, as discussed in Sec. I. As shown in Eqs. (32) and (33), the output noise levels in the amplification region have the same magnitude as the input noise levels. Similarly, using Eq. (23) for the high frequency regime:

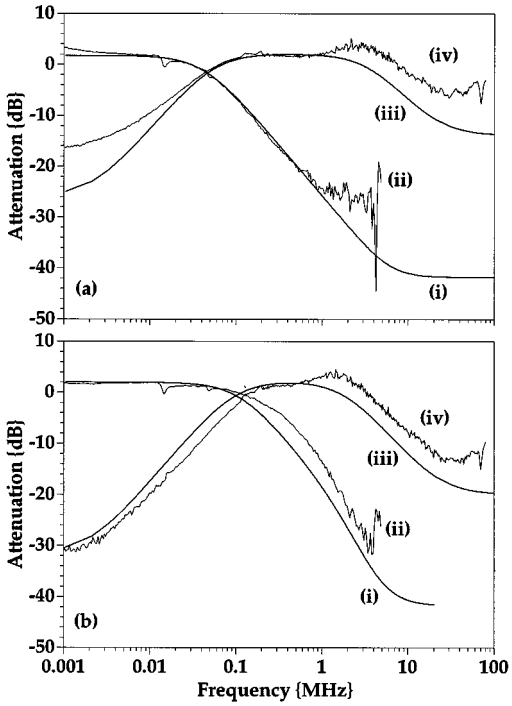

FIG. 10. The transfer functions. (a) shows the noise for the case $H=12.5$ and (b) shows the noise for the case where $H=75$. (i) and (iii) show the theoretical predictions for the slave and master transfer functions, whereas (ii) and (iv) show the experimentally measured transfer functions. In this case, 0 dB implies that the measured noise levels have equal rf powers for the same detected optical photocurrent.

$$V_{\mathrm{obs},l}=1+\eta_2(V_{\mathrm{in}}-1)$$
$$\cong \eta_2 V_{\mathrm{in}}, \quad V_{\mathrm{in}}\gg 1, \tag{34}$$

i.e., at high frequencies the output noise level is lower than the input noise level by the power amplification ratio H. We attribute the discrepancy once again to being detuned from slave cavity resonance and imperfect mode matching [17]. Using Eq. (24) for the low frequency regime:

$$V_{\mathrm{obs},l}=1+\eta_2\left(\frac{V_{\mathrm{in}}}{H}-1\right)$$
$$\cong \eta_2\frac{V_{\mathrm{in}}}{H}, \quad V_{\mathrm{in}}\gg V_p,1, \tag{35}$$

i.e., at low frequency the output noise level tends to a level that is lower than the input noise level by the power amplification ratio squared, H^2. Note that these ideal attenuations are not achievable experimentally due to the presence of other noise sources.

V. DISCUSSION

Our results have shown the basic properties of the injection-locked process, and how the intensity noise from the master and slave lasers passes through to the output of the injection-locked laser. We also observed several features, for example, the full spectral shape of the transfer functions, the amplification of master phase noise by the slave laser,

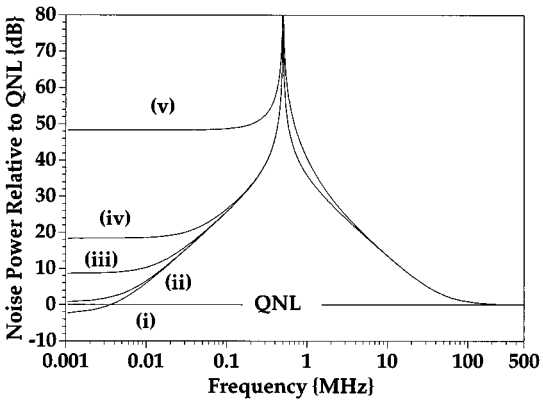

FIG. 11. Theoretical simulation of intensity-noise spectrum for the free-running laser with varying levels of pump noise. The RRO frequency is arbitrarily chosen to be 500 kHz, and all the other constants are as for the slave laser system. (i) shows the noise when the pump is squeezed ($V_p=-10$ dB); (ii) shows the noise when the pump is at QNL ($V_p=0$ dB); (iii) $V_p=10$ dB; (iv) $V_p=20$ dB; (v) $V_p=50$ dB as for the slave laser in these experiments.

and the individual noise sources that influence the output of the locked laser. Furthermore, we have shown that our theoretical model correctly predicts the spectral noise behavior of both the free-running and injection-locked laser systems for all signal powers.

Having verified our model we can now use it to examine the differences between a QNL laser operating at a given output power and an injection-locked laser at the same power. In this comparison we include the possibility that the master and slave pump lasers can operate in a regime where their output is squeezed.

A. Free-running noise spectrum as a function of V_p

Before examining the injection-locked laser let us first inspect the noise spectrum of a solid-state laser when it is free running as the benchmark. Figure 11 shows the output noise level for the free-running slave laser, V_f, for varying amounts of pump noise V_p. The simulation shows V_f for a fixed output power of that laser system relative to QNL. In this notation, the spectrum of a QNL laser is at 0 dB. A laser that has an output noise level below 0 dB exhibits sub-Poissonian statistics, i.e., squeezed, whereas a laser that has an output noise level which is above 0 dB has super-Poissonian statistics.

We have chosen the RRO frequency to be approximately 500 kHz for simplicity. For all the simulations presented we model the input noise to be white in nature and the noise level is referred to the QNL. Hence 0 dB indicates that the noise level is equal to QNL (i.e., $V=1$).

Figure 11 shows that the RRO is present for all pump noise levels, even if the slave pump source is squeezed, i.e., $V_p=0.1$ in this case. This is because the RRO is driven by vacuum fluctuations and hence is present in the intensity-noise spectrum irrespective of the magnitude of the other noise sources. If the pump is squeezed then the free-running laser produces a squeezed output at frequencies near dc. This effect has been observed in diode lasers pumped with sub-Poissonian currents [10]. As the pump noise increases we

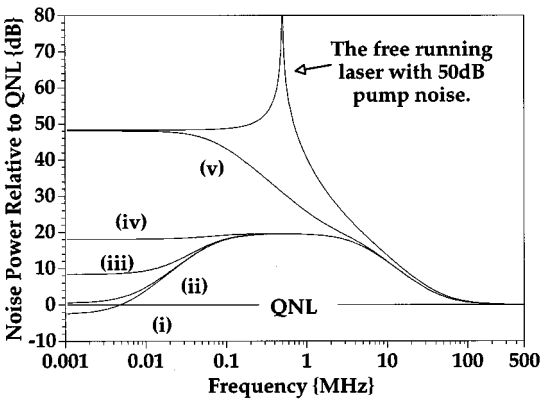

FIG. 12. Theoretical simulation of intensity-noise spectrum for the injection-locked laser with varying levels of slave laser pump noise, and $V_{\text{in}}=0$ dB. (i) shows the noise when the pump is squeezed ($V_p=-10$ dB); (ii) shows the noise when the pump is at QNL ($V_p=0$ dB); (iii) $V_p=10$ dB; (iv) $V_p=20$ dB; (v) $V_p=50$ dB. The RRO of Fig. 11(v) is also shown for reference.

obtain an intensity-noise spectrum similar to that shown in Fig. 5. Note that there is minimal change in the intensity-noise spectrum near the RRO frequency as we increase the pump noise.

B. Injection-locked noise profile as a function of V_p and V_{in}

In Figs. 12 and 13 we show simulations of the noise level for the injection-locked system for varying amounts of slave pump noise and master laser noise levels, respectively. We have chosen the amplification ratio to be fixed at $H=10$.

Illustrated in Fig. 12 is the variation of V_l for the situation where the master laser noise level is at the QNL, i.e., $V_{\text{in}}=1=0$ dB, and the slave pump noise level is varied. It is evident from this diagram that the slave pump noise has the greatest influence on V_l in the frequency region below the amplification region. In the case of sub-Poissonian slave pump noise ($V_p=0.1=-10$ dB) we find that V_l is sub-Poissonian in the frequency regime below the amplification region. The sub-Poissonian behavior is lost once the amplification region is reached, and beyond. This implies that the statistics of the slave pump source are not destroyed by the injection locking process provided that we are in the frequency regime below the amplification region, thus the signal to noise ratio can be better than that of a QNL laser of the same power. This effect has been observed in independent experiments using diode lasers [22]. Note that in general free-running diode lasers do not produce a squeezed output when their pump current is sub-Poissonian due to the existence of near threshold modes that beat with the main lasing mode to cause excess noise. The injected field acts to suppress all these extra modes and hence recover the squeezing [13]. As V_p is increased then there is a corresponding increase in V_l, however, the noise increase is primarily restricted to the low frequency regime. Note that V_l is always within the noise profile of V_f, Fig. 12(v).

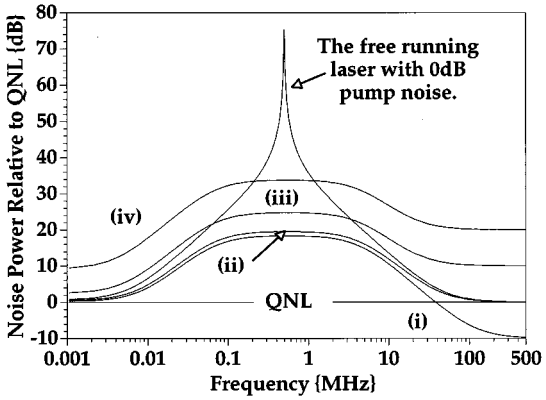

FIG. 13. Theoretical simulation of intensity-noise spectra for the injection-locked laser with varying levels of master noise, and $V_p=0$ dB. (i) shows the noise when the master is squeezed ($V_{\text{in}}=-10$ dB); (ii) shows the noise when the master is at QNL ($V_{\text{in}}=0$ dB); (iii) $V_{\text{in}}=10$ dB; (iv) $V_{\text{in}}=20$ dB. The RRO of Fig. 11(ii) is also shown for reference.

The curves in Fig. 13 show V_l as a function of V_{in}, with $V_p=1$. These curves indicate that master laser noise affects the entire spectrum, but has its greatest influence in the frequency regime above the amplification region. In the case of sub-Poissonian master noise ($V_{\text{in}}=0.1$), we find that V_l has sub-Poissonian statistics at frequencies above the amplification region, but not in the amplification region or below. Hence the statistics of the master laser are preserved above the amplification region by the injection locking process. This occurs because the master field is reflected off the slave cavity and then beats with the slave carrier to produce the observed noise level, see Ref. [12] for more details. Hence in the high frequency region the injection-locked laser output can have sub-Poissonian statistics if the master laser is sub-Poissonian, which implies that the signal to noise ratio can be better than that of a QNL high power laser.

From the results above we note that in the amplification region, the noise statistics are never sub-Poissonian. In fact, the injection-locked noise output in this region is shown to be always larger than the QNL irrespective of the input noise levels. This is due to amplification of quantum fluctuations in the injected (master) field, as occurs in optical amplifiers. The implication of this is that the signal to noise ratio in this region will always be worse than that of a QNL high power laser, and thus this region should be avoided when QNL measurements are required.

C. Injection-locked noise profile as a function of amplification factor

The final effect to consider is a variation of the amplification factor H. The effect of H on the noise level can be seen in Fig. 14. In this diagram we show the intensity-noise spectrum for several different power amplification ratios and for the situation where both the master laser and slave pump source are operating at the QNL. It can be seen from the diagrams that the magnitude of V_l increases with increasing H. In the limit of very large H we find that V_l is equal to the free-running slave laser noise profile. The reason for this behavior is that the injection-locked slave laser is less strongly driven by the external field as H increases. The slave laser is then more susceptible to quantum fluctuations and the noise from the injected field. Note that the noise in the amplification region is contained completely within the

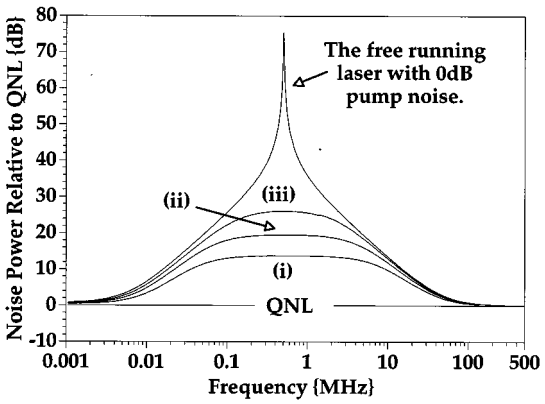

FIG. 14. Theoretical simulation of intensity-noise spectra for the injection-locked laser with varying amplification ratio H, with $V_{\text{in}}=0$ dB and $V_p=0$ dB. (i) shows the noise when ($H=5$); (ii) shows the noise when ($H=25$); and (iii) when ($H=230$). The RRO of Fig. 11(ii) is also shown for reference.

boundaries of the free-running laser's RRO. This is because the same mechanism gives rise to both effects.

VI. CONCLUSION

We have presented experimental and theoretical results that show the qualitative and quantitative behavior of an injection-locked Nd:YAG solid-state laser system. Our experimental results are in excellent agreement with our theoretical predictions. This work extends semiclassical models, which are only valid for large noise levels, to the quantum-noise regime, and predicts behavior at these low noise levels.

We have measured the transfer functions from intensity noise of the slave's pump and the master laser to the injection-locked slave laser and extended the measurements to modulations as low as the QNL. These results show that the noise on the output of the injection-locked laser is dependent on the noise contributed from both the slave's pump and the master laser noise. Outside the amplification region, where the pump and the master contribute independently, squeezed states can be preserved, whereas inside the amplification region the output noise is always greater than QNL. Therefore the injection-locked laser can be better than a QNL laser of the same power under appropriate conditions. The amplification region has to be avoided for any QNL measurement applications.

ACKNOWLEDGMENTS

This work has been a bilateral collaboration funded by the Laser Zentrum Hannover and the Australian Department of Trade and Industry. We would like to thank G. Newton, R. Ballagh, C. Savage, P. Rottengatter, M. Gray, D. Body, A. White, and B. Brown for their assistance and contributions to this work. C.C.H. received financial support from the Australian National University. T.C.R. received financial support from FRST, New Zealand. E.H.H. received financial support from the Australian National University. This project has been financially supported by a grant from the Australian Research Council.

[1] T. C. Ralph, C. C. Harb, and H.-A. Bachor, preceding paper, Phys. Rev. A **54**, 4359 (1996).
[2] A. E. Siegman, *Lasers* (University Science, Mill Valley, CA, 1986).
[3] T. J. Kane and R. L. Byer, Opt. Lett. **10**, 65 (1985).
[4] C. D. Nabors, A. D. Farinas, T. Day, S. D. Yang, E. K. Gustafson, and R. L. Byer, Opt. Lett. **14**, 1189 (1989).
[5] A. D. Farinas, E. K. Gustafson, and R. L. Byer, Opt. Lett. **19**, 114 (1994).
[6] D. Golla, I. Freitag, H. Zellmer, W. Schöne, I. Kröpke, and H. Welling, Opt. Commun. **98**, 86 (1993); I. Freitag, D. Golla, S. Knoke, W. Schöne, H. Zellmer, A. Tünnermann, and H. Welling, Opt. Lett. **20**, 462 (1995).
[7] R. Barillet, *et al.*, Measurement Sci. Technol. **7**, 162 (1996).
[8] I. Freitag and H. Welling, Appl. Phys. B **58**, 537 (1994).
[9] A. D. Farinas, E. K. Gustafson, and R. L. Byer, J. Opt. Soc. Am. B **12**, 328 (1995).
[10] Y. Yamamoto, S. Machida, and O. Nilsson, Phys. Rev. A **34**, 4025 (1986).
[11] L. Gillner, G. Bjork, and Y. Yamamoto, Phys. Rev. A **41**, 5053 (1990).
[12] T. C. Ralph and H.-A. Bachor, Opt. Commun. **119**, 301 (1995).
[13] Note that injection locking is a phenomenon that occurs when the injected master laser mode has a wavelength that lies inside the gain bandwidth of the slave laser and is simultaneously near a longitudinal mode of the slave cavity. Consequently, a slave laser can be injection locked to the master laser even if their wavelength separation is many GHz apart. We were able to lock the slave to the master when the two had wavelength separations greater than 75 GHz. The implication of this is that the injection locking process acts to suppress the free-running slave laser modes and replace them with a new mode which oscillates at the master laser wavelength. We are, however, only considering the case where the master wavelength is the same as the slave wavelength.
[14] H. A. Haus and J. A. Mullen, Phys. Rev. **128**, 2407 (1962).
[15] T. J. Kane, IEEE Photonics Technol. Lett. **2**, 244 (1990).
[16] C. C. Harb, M. B. Gray, H.-A. Bachor, R. Schilling, P. Rottengatter, I. Freitag, and H. Welling, IEEE J. Quantum Electron. **30**, 2907 (1994).
[17] E. Huntington, Honours thesis, The Australian National University, 1995 (unpublished); E. Huntington, C. C. Harb, T. C. Ralph, H.-A. Bachor, and D. E. McClelland (unpublished).
[18] R. W. P. Drever, J. L. Hall, F. W. Kowalski, J. Hough, G. M. Ford, A. J. Munley, and H. Ward, Appl. Phys. B **31**, 97 (1983); A. Schenzle, R. G. DeVoe, and R. G. Brewer, Phys. Rev. A **25**, 2606 (1982).
[19] W. Koechner, *Solid-state Laser Engineering* (Springer-Verlag,

Berlin, 1988). Note, the value given for the stimulated emission rate for Nd:YAG in this book is larger than the excepted value that is quoted in this work.

[20] P. Galatola, L. A. Lugiato, M. G. Porreca, P. Tombesi, and G. Leuchs, Opt. Commun. **85**, 95 (1991).

[21] T. A. B. Kennedy, T. B. Anderson, and D. F. Walls, Phys. Rev. A **40**, 1385 (1989).

[22] S. Inoue, S. Machida, Y. Yamamoto, and H. Ohzu, Phys. Rev. A **48**, 2230 (1993).